Journal for ImmunoTherapy of Cancer

Clinical, FDG-PET and molecular markers of immune checkpoint inhibitor response in patients with metastatic Merkel cell carcinoma

Alison M Weppler ,[1] Andrew Pattison,[2] Prachi Bhave,[1] Paolo De Ieso,[3] Jeanette Raleigh,[1] Athena Hatzimihalis,[1] Anthony J Gill,[4,5] Shiva Balachander,[2] Jason Callahan,[6] Margaret Chua,[3] George Au-Yeung,[1] Grant A McArthur,[1] Rodney J Hicks,[6] Richard W Tothill,[1,2] Shahneen Sandhu[1]

To cite: Weppler AM, Pattison A, Bhave P, *et al*. Clinical, FDG-PET and molecular markers of immune checkpoint inhibitor response in patients with metastatic Merkel cell carcinoma. *Journal for ImmunoTherapy of Cancer* 2020;**8**:e000700. doi:10.1136/jitc-2020-000700

► Additional material is published online only. To view, please visit the journal online (http://dx.doi.org/10.1136/jitc-2020-000700).

AMW, AP, RWT and SS contributed equally.

Accepted 25 August 2020

For numbered affiliations see end of article.

Correspondence to
Dr Shahneen Sandhu; Shahneen.Sandhu@petermac.org

ABSTRACT

Background Metastatic Merkel cell carcinoma (mMCC) is an aggressive neuroendocrine malignancy of the skin with a poor prognosis. Immune checkpoint inhibitors (ICIs) have shown substantial efficacy and favorable safety in clinical trials.

Methods Medical records of patients (pts) with mMCC treated with ICIs from August 2015 to December 2018 at Peter MacCallum Cancer Centre in Australia were analyzed. Response was assessed with serial imaging, the majority with FDG-PET/CT scans. RNA sequencing and immunohistochemistry for PD-L1, CD3 and Merkel cell polyomavirus (MCPyV) on tumor samples was performed.

Results 23 pts with mMCC were treated with ICIs. A median of 8 cycles (range 1 to 47) were administered, with treatment ongoing in 6 pts. Objective responses (OR) were observed in 14 pts (61%): 10 (44%) complete responses (CR) and 4 (17%) partial responses (PR). Median time to response was 8 weeks (range 6 to 12) and 12-month progression-free survival rate was 39%. Increased OR were seen in pts aged less than 75 (OR 80% vs 46%), no prior history of chemotherapy (OR 64% vs 50%), patients with an immune-related adverse event (OR 100% vs 43%) and in MCPyV-negative tumors (OR 69% vs 43%). Pts with a CR had lower mean metabolic tumor volume on baseline FDG-PET/CT scan (CR: 35.7 mL, no CR: 187.8 mL, p=0.05). There was no correlation between PD-L1 positivity and MCPyV status (p=0.764) or OR (p=0.245). 10 pts received radiation therapy (RT) during ICI: 4 pts started RT concurrently (OR 75%, CR 50%), 3 pts had isolated ICI-resistant lesions successfully treated with RT and 3 pts with multisite progression continued to progress despite RT. Overall, 6 pts (26%) had grade 1–2 immune-related adverse events.

Conclusion ICIs showed efficacy and safety in mMCC consistent with trial data. Clinical and imaging predictors of response were identified.

BACKGROUND

Merkel cell carcinoma (MCC) is an aggressive neuroendocrine malignancy of the skin, with a historical 5-year overall survival (OS) rate of 15% to 27% for patients with metastatic disease.[1] Until recently, chemotherapy was the mainstay of treatment for metastatic MCC (mMCC), resulting in a median progression-free survival (PFS) of 3 months.[2] Merkel cell polyomavirus (MCPyV) and ultraviolet (UV) carcinogenesis are implicated in MCC development.[3 4] While both mechanisms drive tumorigenesis, they also induce potent adaptive immune responses to either viral antigens or neoantigens. An increased incidence of MCC in immunosuppressed patients suggests that immune escape is essential for MCC development[5 6] and that targeting immune evasion may be an effective treatment strategy.

Immune checkpoint inhibitors (ICIs) have emerged as an attractive treatment option for patients with mMCC. In the phase II JAVELIN Merkel 200 trial, 88 patients who had failed prior chemotherapy were treated with avelumab, with a response rate (RR) of 33%, 2-year PFS rate of 26% and median duration of response not yet reached.[7] Responses appear to be superior in the first-line setting, with an interim analysis of part B of the Javelin Merkel 200 trial demonstrating an RR of 62% in 39 patients with no prior cytotoxic treatment for metastatic disease.[8] Similar promising results have been seen with other ICIs; pembrolizumab achieved an RR of 56% in the first-line setting in 50 patients with advanced MCC (unresectable: 7, metastatic: 43), with 79% of responders in ongoing remission at 2 years and a 2-year OS rate of 68.7%.[9]

To date, there is limited published experience with ICIs in mMCC outside of a clinical trial setting, in which inclusion criteria, such as performance status and comorbid conditions, are restrictive. Further, predictive markers of response to ICIs in mMCC have

not been well established. Herein, we describe our experience in using ICIs for mMCC as single agent therapy or concurrently with radiation at the Peter MacCallum Cancer Centre (PMCC) in Melbourne, Australia. We outline clinical, imaging and molecular characteristics of treatment response.

METHODS

Study design and participants

All patients with mMCC treated with ICIs from August 1, 2015 to December 31, 2018 at PMCC were prospectively consented for inclusion in a longitudinal MCC biomarker study (HREC number: 14/113). Clinical data including patient demographics, staging, prior treatments, response and toxicity assessments were annotated prospectively. Formalin-fixed paraffin-embedded (FFPE) tissue from a primary or metastatic site was collected for all patients. Most patients had [^{18}F]-fluoro-2-deoxyglucose-PET/CT (FDG-PET/CT) imaging at baseline and every 8–12 weeks to monitor treatment response (n=19), with CT alone used to assess response in a minority of patients (n=4).

Medical records and the study-specific database were retrospectively analyzed to collect information on patient and disease characteristics, treatment course and outcomes. Baseline FDG-PET/CT metabolic tumor volume (MTV) was evaluated by a nuclear medicine technologist (JC) using proprietary software (MIMencore, V.6.7). The MTV was contoured using a patient-specific threshold of 1.5× liver standardized uptake value (SUV) mean+2 standard deviations (SD) of the liver SUV.[10] Manual adjustments were made for disease that was only mildly FDG-avid and fell below this threshold in consultation with an experienced FDG-PET/CT reader (RJH). Response evaluation was undertaken with PET Response Criteria in Solid Tumors (PERCIST) criteria for FDG-PET/CT[10] and Response Evaluation Criteria in Solid Tumors (RECIST) 1.1 for CT scans.[11] For convenience of reporting overall response rates, metabolic response criteria of complete and partial metabolic response (CMR and PMR) were combined with morphologic responses of complete and partial responses (CR and PR), respectively.

Immunohistochemistry (IHC)

IHC was performed on 4 µm FFPE sections. MCPyV (clone CM2B4; cat sc-136172, Santa Cruz Biotechnology, Santa Cruz, CA; dilution 1:100) and CD3 (clone LN10; cat NCL-L-CD3-565, Newcastle, UK; dilution 1:200) staining was performed on the Leica Bond III Autostainer. For programmed death-ligand 1 (PD-L1), IHC clone SP263 was used (Assay v1.00.0001, using the VENTANA OptiView DAB IHC Detection Kit on the BenchMark ULTRA autostainer). Semiquantitative scoring was performed by a single pathologist blinded to the clinical data. T cells were scored by counting the mean number of positive cells in tumor per high-power field (0.55 mm diameter). PD-L1 scoring was performed using a standardized approach that has been described previously.[12] Briefly, two scores were derived; the tumor proportion score (TPS), which represents the percentage of tumor cells showing positive membranous expression of PD-L1, and the immune cell score (IC), which represents the proportion of tumor area occupied by PD-L1–positive immune cells. TPS and IC assessment was based on the entire tumor area on a single representative slide. A minimum of 50 tumor cells were required for a tumor to be considered assessable for TPS and IC. Four and three patients did not have sufficient material for PD-L1 and CD3 IHC, respectively, and were excluded from this analysis.

RNA-sequencing (RNA-Seq)

RNA was prepared using the NEBNext Ultra II Directional RNA Library Prep Kit for Illumina and libraries sequenced on the Illumina Nova-Seq 6000. For details on RNA-Seq bioinformatic analysis, including differential gene expression, gene set enrichment analysis, confirmation of viral status and variant calling, see the online supplemental methods. Three patients did not have sufficient material for RNA-Seq and were excluded from this analysis.

Statistical analysis

Baseline characteristics were summarized using standard descriptive statistics. Bivariate analyses using χ^2 tests were used to compare treatment response by clinical and disease-specific biomarkers, including baseline FDG-PET/CT MTV. Univariable Cox proportional hazard regression was used to assess the association between CMR on early FDG-PET/CT scan and PFS and OS. All statistical analyses were performed using STATA (StataCorp. 2017. *Stata Statistical Software: Release 15*. College Station, TX: StataCorp LLC).

RESULTS

Twenty-three patients with mMCC with a median age of 75 years (range 64 to 91) were treated with ICIs, with two-thirds (n=15, 65%) receiving treatment with the PD-L1 inhibitor avelumab. Ten patients (43%) had received prior chemotherapy, all within 6 months of starting ICI (4: adjuvant chemotherapy, 6: first-line treatment for mMCC). Baseline characteristics are summarized in table 1.

Clinical experience

A median of 8 cycles (range 1 to 47) of ICI were administered, with treatment ongoing in six patients. Objective responses (OR) were observed in 14 patients (61%), with CR as best response in 10 patients (44%) and PR in 4 patients (17%). Median time to response was 8 weeks (range 6 to 12), with all responders demonstrating a response on their first on-treatment scan. Median duration of response is not yet reached (95% CI 21 months to not reached). Twelve-month PFS rate was 39% for the entire cohort. Seventeen patients (74%) discontinued treatment: nine for progressive disease (PD), five for a

Table 1 Baseline characteristics

	N (%)
Age (years)	
Median (range)	75 (64 to 91)
Sex	
Male	18 (78)
Female	5 (22)
ECOG Performance Status	
0	8 (35)
1	12 (52)
2	3 (13)
Ethnicity	
Caucasian	19 (83)
Mediterranean	3 (13)
Pacific Islander	1 (4)
Site of primary tumor	
Head and neck	6 (26)
Upper limb	5 (22)
Lower limb	4 (17)
Trunk	1 (4)
Unknown	7 (30)
ICI	
Avelumab (PD-L1 inhibitor)	15 (65)
Pembrolizumab (PD-1 inhibitor)	5 (22)
Tislelizumab (PD-1 inhibitor)	3 (13)
MCPyV status	
Positive	7 (30)
Negative	16 (70)
Presence of visceral disease	17 (74)
Prior platinum-based chemotherapy	10 (43)
Prior immunosuppression	2 (9)
History of autoimmune disease	2 (9)

ECOG, Eastern Cooperative Oncology Group; ICI, immune checkpoint inhibitor; MCPyV, Merkel cell polyomavirus.

treatment break given CR or stable PR, and three due to deterioration from a comorbid illness. The five patients who discontinued treatment in a CR or PR have maintained their response after an average of 8 months from treatment cessation.

Six patients (26%) had an immune-related adverse event (irAE), all of which were grade 1–2 (two maculopapular rash, one lichenoid rash, one Sweet's syndrome, one arthritis, one hypothyroidism). All patients with an irAE had a response to ICI, with 5 of 6 (83%) achieving a CR. Two patients had a prior history of an autoimmune disease (rheumatoid arthritis) and were successfully treated with ICIs with no flare of their pre-existing condition and no irAEs.

Ten patients (43%) received radiation therapy (RT) during ICI treatment. Four patients received a palliative dose of RT (dose: 20 Gray (Gy) in 5 fractions) to a single site of disease concurrent with commencing ICI, with an OR of 75% and CR of 50%. Three patients had isolated ICI-resistant lesions treated with RT (dose: 20 Gy in 5 fractions), with a response at the irradiated site, allowing them to continue on ICI. This included a patient with a partial response elsewhere and an isolated progressive adrenal metastasis, a patient who achieved a CMR and then demonstrated oligoprogression in a liver lesion, and a patient who achieved a CMR apart from an ICI-resistant left cheek lesion. Three patients with globally progressive disease exhibited a response at the irradiated site but ongoing progressive disease elsewhere. Of note, only 2 (20%) patients who received RT during ICI treatment had an irAE, similar to the toxicity rate in the general cohort.

Clinical and FDG-PET/CT markers of ICI response

Increased OR was seen in patients aged less than 75 years (OR 8/10, 80% vs 46%), no history of prior chemotherapy (OR 9/14, 64% vs 50%), patients with an irAE (OR 6/6, 100% vs 47%) and in MCPyV-negative patients (OR 11/16, 69% vs 43%). These differences were not statistically significant, likely due to small patient numbers. For the 19 patients in whom FDG-PET/CT was used for response assessment, patients with a CMR had lower MTV on baseline scan (CMR: 35.7 mL, no CMR: 187.8 mL; p=0.05) (figure 1). Similarly, CMR on early FDG-PET/CT scan (performed within 12 weeks of ICI initiation) may be a surrogate for PFS (HR 0.31; p=0.38) and OS (HR 0.24; p=0.19), although this trend needs to be confirmed with greater patient numbers.

Molecular markers of ICI response

No correlation was seen between IHC tumor PD-L1 positivity and MCPyV status (p=0.764) or response to ICI (p=0.245). Similarly, no significant association was seen between ICI response and number of $CD3^+$ T cells within the tumor, with an unexpected trend toward higher T-cell infiltration in non-responders (p=0.066).

RNA-Seq confirmed the previously established hallmarks of MCC subtypes. Elevated MCPyV transcripts were restricted to MCPyV-positive tumors (validating MCPyV IHC), while MCPyV-negative tumors had higher tumor mutational burden (TMB) and characteristic UV-mutation signatures (COSMIC v3 Sig7a/b) (figure 2, i–iii). Consistent with results from IHC scoring (figure 2, iv), there was no association between ICI response and the averaged gene expression of immune cell type specific markers (figure 3A) identified from a large compendium of other cancer transcriptomic data (online supplemental table S1).[13] Similarly, no association was observed between ICI response and antigen presentation machinery or PD1/PD-L1 mRNA expression (figure 3B).

Differential expression analysis was done by comparing responders to non-responders while accounting for the

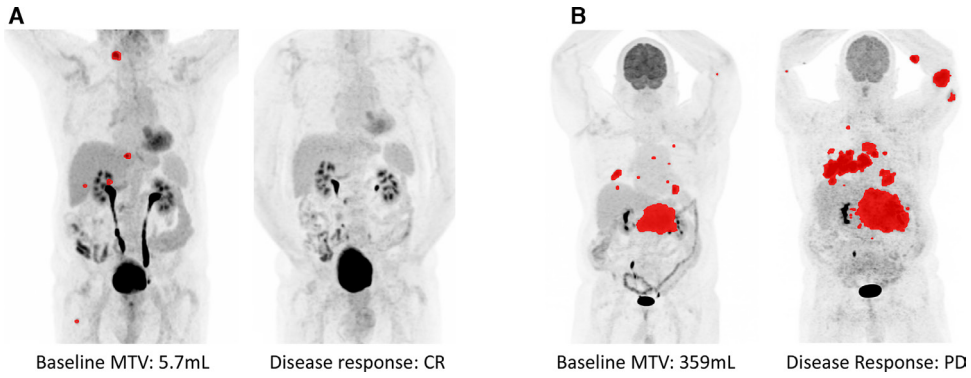

Figure 1 Baseline FDG-PET/CT metabolic tumor volume. (A) Patient 113 with baseline metabolic tumor volume (MTV) of 5.7 mL had a complete response to immune checkpoint inhibitor (ICI). (B) Patient 110 with baseline MTV of 359 mL had primary refractory disease and progressed through ICI.

effect of viral status. Only two genes were found to be significantly differentially expressed (*COL9A3* and *KIF19*, false discovery rate (FDR)<0.05). Neither gene has any known biological relevance to ICI response, T-cell function or the biology of MCC. On the contrary, gene set enrichment analysis identified 7 significantly enriched (FDR<0.05) hallmark gene sets (online supplemental table S2) and 74 gene ontology (GO) gene sets (online supplemental table S3). Gene sets downregulated in the responders (compared with non-responders) included Hallmark gene sets E2F targets, MYC targets (v1) and Oxidative Phosphorylation as well as GO gene sets

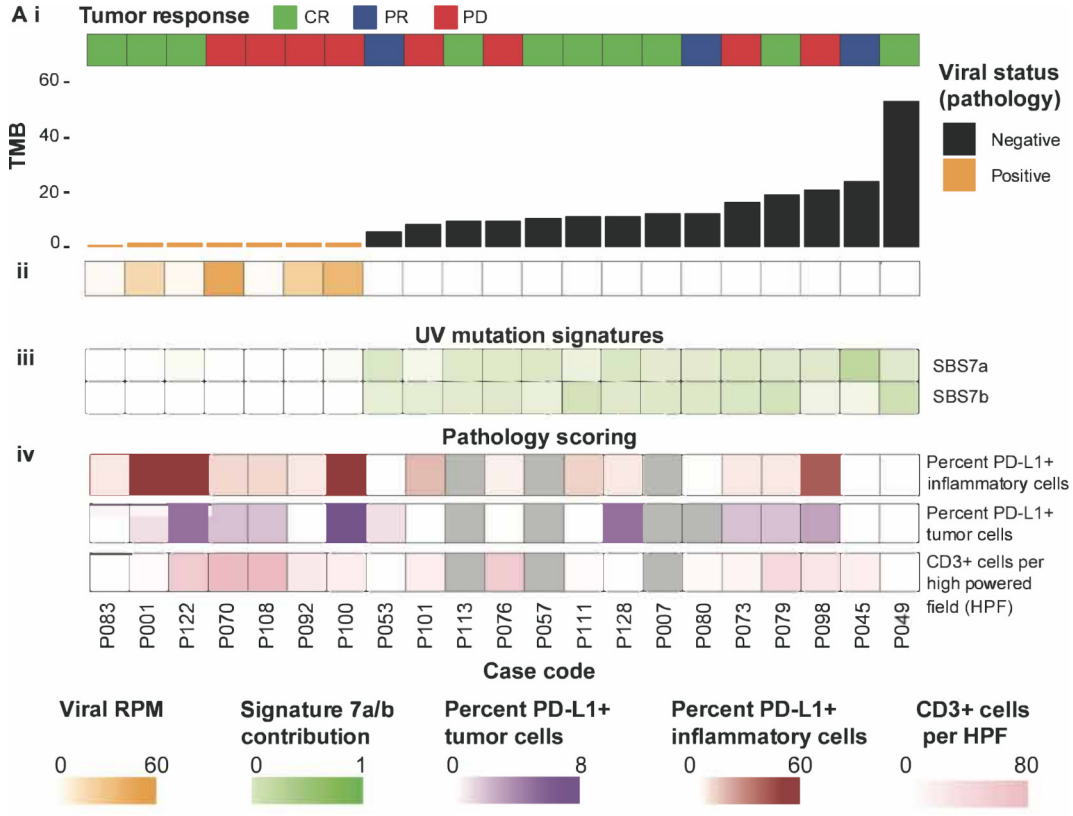

Figure 2 Immunotherapy response, TMB, viral status, UV-associated mutation signatures and PD-L1/CD3$^+$ staining of the cohort. (i) The tumor mutational burden (TMB) calculated from RNA-Seq for each of the samples. Samples are ordered by TMB in this panel and throughout the rest of the figure. Samples are colored by viral status determined from viral antibody staining. The heatmap below (ii) shows the number of viral reads present in each sample as determined by *Xenomapper*[30] divided by the number of mapped reads in each library multiplied by 1×10^6 (RPM). (iii) The relative contribution of UV-associated mutation signatures 7a and 7b to each sample in the cohort. Mutation signatures were generated for each sample in the cohort using *MutationalPatterns*.[31] Samples were compared against single bases substitution (SBS) signatures from COSMIC v3.[32 33] (iv) Pathology scoring of the percentage of PD-L1 positive tumor and immune cells from immunohistochemical staining of each sample as well as the number of CD3$^+$ cells per high-power field studied. CR, complete response; PD, progressive disease; PR, partial response.

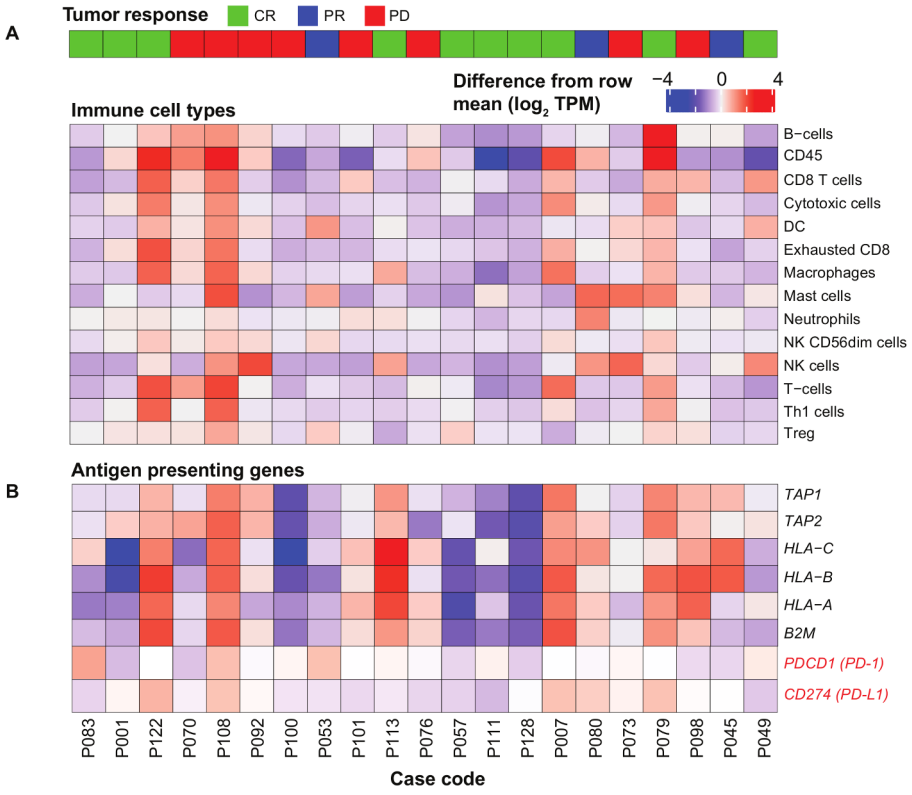

Figure 3 Immune landscape of the cohort. (A) The expression of genes suggested to be associated with particular immune cell types.[13] (B) The expression of genes known to be associated with antigen presentation machinery. The expression of PD-1 (*PDCD1*) and PD-L1 (*CD274*) is highlighted in red. Both panels are mean centered $\log_2$ (TPM+1). CR, complete response; PD, progressive disease; PR, partial response.

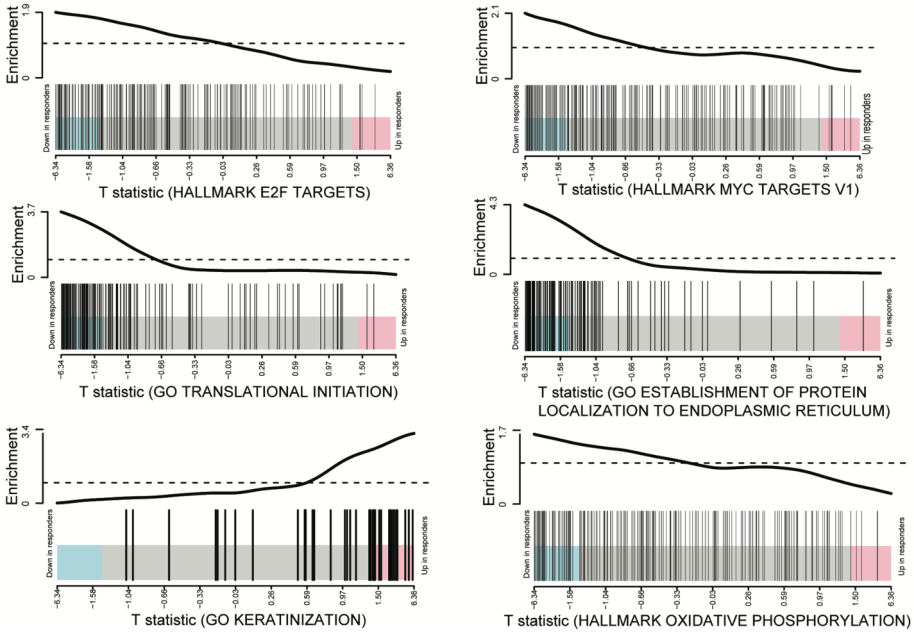

Figure 4 Barcodeplots highlighting lower cellular growth markers in responders. *Limma* barcodeplots of the "E2F targets" and "MYC targets (V1)" gene sets from the MSigDB. There is a clear reduction in the expression of many of the genes in these gene sets in tumors that responded to immune checkpoint inhibitor, suggesting lower proliferation in these samples. *Limma* barcodeplots of the "GO translational initiation" and "GO establishment of protein localisation to the endoplasmic reticulum" gene sets from the MSigDB. These gene sets again highlight a signature of reduced proliferation in responders.

of translational initiation and protein localization to endoplasmic reticulum (figure 4). Gene sets upregulated in responders were associated with keratinocyte differentiation.

DISCUSSION

Consistent with clinical trial data, the majority of patients (61%) responded to ICIs and these responses were notable for their durability, including ongoing disease remission after treatment cessation. Treatment was well tolerated in this elderly population, with no treatment-related deaths or discontinuation due to toxicity. This included patients who received concurrent RT during ICI therapy. Our experience highlights the safety and potential efficacy of combining ICIs and RT, both to enhance initial response and to manage oligoresistant lesions.

We identified clinical and imaging factors associated with increased responses, including lack of prior chemotherapy, younger age, MCPyV-negative tumors, lower baseline FDG-PET/CT MTV and development of treatment-related irAEs. The correlation between irAEs and improved response to ICIs is consistent with other tumor types,[14–16] particularly with respect to cutaneous side effects, which comprised half of the toxicity seen in our cohort. However, this association has not previously been reported with MCC.

While previous studies have not found a statistically significant difference in ICI response based on MCPyV status,[9] our cohort and others indicate that MCPyV-negative mMCC may have an enhanced response to ICIs,[17] potentially attributed to higher TMB,[17 18] a phenomenon described in multiple tumor types.[19] MCPyV-negative MCCs have been found to harbor more tumor neoantigens than melanoma,[18] a cancer highly responsive to ICI. A recent study that characterized the genomic landscape of 317 MCC tumors confirmed a bimodal distribution of TMB, with a strong negative association between TMB and MCPyV DNA.[17] However, despite the likelihood of neoantigens being the major driver of immunogenicity in MCPyV-negative tumors, we did not see a correlation between TMB and ICI response within the MCPyV-negative tumors. This may be due to an insufficient number of cases for analysis or that ICI response in MCPyV-negative tumors is dependent on additional tumor intrinsic and/or extrinsic factors.

To our knowledge, this is the first study to identify a significant association between baseline FDG-PET/CT MTV and response to ICI in mMCC. FDG-PET/CT scans have been shown to be a sensitive and reliable imaging modality to stage patients with mMCC and assess treatment response. Further, a metabolic response on FDG-PET/CT has been shown to be significantly associated with overall survival in patients with mMCC.[20 21] Previous studies have noted a trend toward increased response rates in patients with lower disease burden, as defined by the sum of the target lesion diameters,[7] which is substantiated by our results. These findings mirror results from other cancers, particularly melanoma, where lower baseline tumor burden has been shown to be associated with both response to ICI and improved survival.[22 23] This may be related to increased tumor heterogeneity with high-volume disease, with the former associated with less tumor immune cell infiltration and reduced activation of the immune response.[24] Increased tumor cell volume may also contribute to enhanced secretion of cytokines stimulating regulatory T-cell development in the tumor microenvironment (TME),[25] with a corresponding inhibitory effect on response to ICI. The presence of increased hypoxia in the TME of larger lesions may also be immunosuppressive.[26 27] Overall, this finding underscores a potential benefit of routine surveillance imaging following treatment of early-stage MCC to enable earlier detection of lower volume recurrence, particularly during the first 2 years after locoregional treatment when risk of recurrence is highest.[1]

Identification of reliable biomarkers to predict ICI response in MCC has thus far proven challenging. In our cohort, we found several outlier cases that do not support the notion of increased ICI response corresponding to an inflamed TME. Patient P108 did not respond to ICI, despite having a highly inflamed tumor with strong expression of immune markers. The tumor biopsy was taken prior to treatment with chemotherapy; therefore, we cannot exclude the possibility that chemotherapy altered the immune profile of the tumor. In contrast, five patients (P001, P057, P083, P111, P128) with low expression of immune markers responded to ICI. The average MTV for four of these patients with baseline FDG-PET/CT scans was 29.49 mL, which was significantly lower than the general cohort ($p<0.01$), further supporting the finding that low-volume disease is an important factor in predicting robust responses to ICI, even in patients without an inflamed tumor phenotype.

RNA-Seq analysis identified a number of gene sets enriched in non-responders indicating increased ribogenesis, translational initiation and post-translational processing as well as upregulation of cell cycle checkpoints. These results are in keeping with increased cell growth and proliferation of tumor cells in the non-responders. ICI responders conversely had upregulation of gene sets associated with keratinocyte differentiation, which is intriguing considering that epidermal keratinocyte precursor cells are hypothesized to be a putative MCC cell of origin.[28] Upregulation of a hallmark gene set of oxidative phosphorylation in the non-responders may indicate a higher level of aerobic metabolism in this group, which is consistent with a recent study reporting oxidative metabolism as a barrier to PD-1 blockade in other tumor types.[27] The gene sets identified in this study will require validation in an independent MCC patient cohort, but they highlight potential resistance mechanisms to ICIs in this disease and point to opportunities for rational drug combinations to overcome this resistance. For example, metformin inhibits mitochondrial complex I and has been shown to decrease tumor oxygen

consumption rate in preclinical models, with this reduction in tumor oxidative phosphorylation signaling able to remodel the hypoxic TME and enhance response to ICIs.[29]

This study is limited by the retrospective nature, although annotation of toxicity was undertaken prospectively and calculation of baseline MTV was done independent of medical records by a single molecular imaging technologist and independently reviewed by an expert with over 30 years of experience in PET imaging to ensure accuracy and consistency. A larger sample size would be needed to more formally assess for statistical significance of the trends noted in our cohort. Ongoing research with ICI therapy in patients with mMCC should focus on elucidating markers of response as well as investigating rational treatment combinations.

CONCLUSION

In this study, ICIs showed efficacy and safety in mMCC consistent with trial data, with durable responses that persisted even after treatment discontinuation. Clinical and imaging predictors of response were identified. While no clear molecular biomarker emerged, RNA-sequencing identified gene sets enriched in non-responders, identifying potential resistance mechanisms that warrant additional evaluation.

Author affiliations
[1]Department of Medical Oncology, Peter MacCallum Cancer Centre, Melbourne, Victoria, Australia
[2]Department of Clinical Pathology and Centre for Cancer Research, University of Melbourne, Melbourne, Victoria, Australia
[3]Department of Radiation Oncology, Peter MacCallum Cancer Centre, Melbourne, Victoria, Australia
[4]Cancer Diagnosis and Pathology Group, Kolling Institute of Medical Research, Royal North Shore Hospital, Sydney, New South Wales, Australia
[5]Department of Anatomical Pathology, University of Sydney, Sydney, New South Wales, Australia
[6]Department of Molecular Imaging and Therapeutic Nuclear Medicine, Peter MacCallum Cancer Centre, Melbourne, Victoria, Australia

Contributors AMW collated the clinical data, performed statistical analysis and was a major contributor in writing the manuscript. AP performed the RNA-sequencing and differential gene expression analysis and was a major contributor in writing the manuscript. SB helped with the translational aspects of the study. PB collated the clinical data and contributed in writing the manuscript. JR and AH prospectively consented patients to the study and collected biospecimens and clinical data. AJG performed IHC analysis on the samples. JC and RJH collected the FDG-PET/CT data and calculated baseline FDG-PET/CT MTV. PDI, MC, GA-Y and GAM contributed to the study concept and contributed in writing the manuscript. SS oversaw the study and data collection and was a major contributor in writing the manuscript. RWT led the translational aspects of the study and was a major contributor in writing the manuscript. All authors read and approved the final manuscript.

Funding The authors have not declared a specific grant for this research from any funding agency in the public, commercial or not-for-profit sectors.

Competing interests None declared.

Patient consent for publication Not required.

Ethics approval This study was approved by the Peter MacCallum Cancer Centre Human Research Ethics Committee (HREC no. 14/113). All patients were prospectively consented to participate in the study.

Provenance and peer review Not commissioned; externally peer reviewed.

Data availability statement Data are available on reasonable request.

ORCID iD
Alison M Weppler http://orcid.org/0000-0003-3769-490X

REFERENCES

1 Harms KL, Healy MA, Nghiem P, *et al*. Analysis of prognostic factors from 9387 Merkel cell carcinoma cases forms the basis for the new 8th edition AJCC Staging System. *Ann Surg Oncol* 2016;23:3564–71.
2 Iyer JG, Blom A, Doumani R, *et al*. Response rates and durability of chemotherapy among 62 patients with metastatic Merkel cell carcinoma. *Cancer Med* 2016;5:2294–301.
3 Wong SQ, Waldeck K, Vergara IA, *et al*. UV-associated mutations underlie the etiology of MCV-negative Merkel cell carcinomas. *Cancer Res* 2015;75:5228–34.
4 Feng H, Shuda M, Chang Y, *et al*. Clonal integration of a polyomavirus in human Merkel cell carcinoma. *Science* 2008;319:1096–100.
5 Femia D, Prinzi N, Anichini A, *et al*. Treatment of advanced Merkel cell carcinoma: current therapeutic options and novel immunotherapy approaches. *Target Oncol* 2018;13:567–82.
6 Shirley M. Avelumab: a review in metastatic Merkel cell carcinoma. *Target Oncol* 2018;13:409–16.
7 Kaufman HL, Russell JS, Hamid O, *et al*. Updated efficacy of avelumab in patients with previously treated metastatic Merkel cell carcinoma after ≥1 year of follow-up: JAVELIN Merkel 200, a phase 2 clinical trial. *J Immunother Cancer* 2018;6:7.
8 D'Angelo SP, Russell J, Lebbé C, *et al*. Efficacy and safety of first-line avelumab treatment in patients with stage IV metastatic Merkel cell carcinoma: a preplanned interim analysis of a clinical trial. *JAMA Oncol* 2018;4:e180077.
9 Nghiem P, Bhatia S, Lipson EJ, *et al*. Durable tumor regression and overall survival in patients with advanced Merkel cell carcinoma receiving pembrolizumab as first-line therapy. *J Clin Oncol* 2019;37:693–702.
10 Wahl RL, Jacene H, Kasamon Y, *et al*. From RECIST to PERCIST: evolving considerations for PET response criteria in solid tumors. *J Nucl Med* 2009;50 Suppl 1:122S–50.
11 Eisenhauer EA, Therasse P, Bogaerts J, *et al*. New response evaluation criteria in solid tumours: revised RECIST guideline (version 1.1). *Eur J Cancer* 2009;45:228–47.
12 Tsao MS, Kerr KM, Kockx M, *et al*. PD-L1 immunohistochemistry comparability study in real-life clinical samples: results of Blueprint Phase 2 Project. *J Thorac Oncol* 2018;13:1302–11.
13 Danaher P, Warren S, Dennis L, *et al*. Gene expression markers of tumor infiltrating leukocytes. *J Immunother Cancer* 2017;5:18.
14 Hua C, Boussemart L, Mateus C, *et al*. Association of vitiligo with tumor response in patients with metastatic melanoma treated with pembrolizumab. *JAMA Dermatol* 2016;152:45–51.
15 Sanlorenzo M, Vujic I, Daud A, *et al*. Pembrolizumab cutaneous adverse events and their association with disease progression. *JAMA Dermatol* 2015;151:1206–12.
16 Freeman-Keller M, Kim Y, Cronin H, *et al*. Nivolumab in resected and unresectable metastatic melanoma: characteristics of immune-related adverse events and association with outcomes. *Clin Cancer Res* 2016;22:886–94.
17 Knepper TC, Montesion M, Russell JS, *et al*. The genomic landscape of Merkel cell carcinoma and clinicogenomic biomarkers of response to immune checkpoint inhibitor therapy. *Clin Cancer Res* 2019;25:5961–71.
18 Goh G, Walradt T, Markarov V, *et al*. Mutational landscape of MCPyV-positive and MCPyV-negative Merkel cell carcinomas with implications for immunotherapy. *Oncotarget* 2016;7:3403–15.
19 Yarchoan M, Hopkins A, Jaffee EM. Tumor mutational burden and response rate to PD-1 inhibition. *N Engl J Med* 2017;377:2500–1.
20 Byrne K, Siva S, Chait L, *et al*. 15-Year experience of 18F-FDG PET imaging in response assessment and restaging after definitive treatment of Merkel cell carcinoma. *J Nucl Med* 2015;56:1328–33.
21 Ben-Haim S, Garkaby J, Primashvili N, *et al*. Metabolic assessment of Merkel cell carcinoma: the role of 18F-FDG PET/CT. *Nucl Med Commun* 2016;37:865–73.

22 Robert C, Ribas A, Hamid O, *et al*. Durable complete response after discontinuation of pembrolizumab in patients with metastatic melanoma. *J Clin Oncol* 2018;36:1668–74.
23 Joseph RW, Elassaiss-Schaap J, Kefford R, *et al*. Baseline tumor size is an independent prognostic factor for overall survival in patients with melanoma treated with pembrolizumab. *Clin Cancer Res* 2018;24:6098–67.
24 McDonald K-A, Kawaguchi T, Qi Q, *et al*. Tumor heterogeneity correlates with less immune response and worse survival in breast cancer patients. *Ann Surg Oncol* 2019;26:2191–9.
25 Landskron G, De la Fuente M, Thuwajit P, *et al*. Chronic inflammation and cytokines in the tumor microenvironment. *J Immunol Res* 2014;2014:1–19.
26 Lequeux A, Noman MZ, Xiao M, *et al*. Impact of hypoxic tumor microenvironment and tumor cell plasticity on the expression of immune checkpoints. *Cancer Lett* 2019;458:13–20.
27 Najjar YG, Menk AV, Sander C, *et al*. Tumor cell oxidative metabolism as a barrier to PD-1 blockade immunotherapy in melanoma. *JCI Insight* 2019;4. doi:10.1172/jci.insight.124989. [Epub ahead of print: 07 Mar 2019].
28 Tilling T, Moll I. Which are the cells of origin in Merkel cell carcinoma? *J Skin Cancer* 2012;2012:1–6.
29 Scharping NE, Menk AV, Whetstone RD, *et al*. Efficacy of PD-1 blockade is potentiated by metformin-induced reduction of tumor hypoxia. *Cancer Immunol Res* 2017;5:9–16.
30 J. Wakefield M. Xenomapper: mapping reads in a mixed species context. *JOSS* 2016;1:18.
31 Blokzijl F, Janssen R, van Boxtel R, *et al*. MutationalPatterns: comprehensive genome-wide analysis of mutational processes. *Genome Med* 2018;10:33.
32 Alexandrov L, Kim J, Haradhvala NJ, *et al*. The repertoire of mutational signatures in human cancer. *BioRxiv* 2018:322859.
33 Tate JG, Bamford S, Jubb HC, *et al*. COSMIC: the catalogue of somatic mutations in cancer. *Nucleic Acids Res* 2019;47:D941–7.

Supplementary methods

Read alignment and quantification

FASTQ files were aligned with *STAR* (version 2.6.1d) to the human genome (version GRCh37) to generate bam files[1]. Gene expression quantification was performed with *Salmon* (version 0.12)[2]. Raw genewise counts to be used in downstream analyses were extracted as length scaled TPM values from *Salmon* outputs using the *Tximport* R package (version 1.12.0)[3].

Gene expression analysis

DGE analysis was performed with the *Limma* R package (version 3.40.2)[4]. GSEA was performed with *CAMERA*[5] using the hallmark and gene ontology (GO) gene sets from the Molecular Signatures Database (MSigDB)[6].

Confirmation of tumor viral status

Tumor viral status was confirmed by running *Xenomapper* against the MCPyV (NCBI Reference Sequence: NC_010277.2) and human genome (GRCh37).

Variant calling from RNA-Seq

Variants were called using a modified version of the GATK best practices for variant calling from RNA-Seq (https://gatkforums.broadinstitute.org/gatk/discussion/3892/the-gatk-best-practices-for-variant-calling-on-rnaseq-in-full-detail), with the exception that GATK version 4 rather than 3 was used (GATK version 4.1.0.0)[7 8]. Variants were also called using *VarScan* (version 2.4.3)[9] with a minimum of 8 bases of coverage and 3 bases supporting each variant call. To be considered a true call, the variant had to be called by both the GATK

HaploypeCaller and *VarScan*. To filter out germline variants, all variants present in the dbSNP (version 151) were removed and additionally any variant present in more than 20% of the cohort was removed. To remove mutations caused by RNA-editing, any sites present in the RADAR RNA-editing database[10] were also removed. The method was originally developed using 167 lung squamous cell carcinoma (LUSC) RNA-Seq samples from the TCGA with matched whole exome sequencing (WES) data. The method was able to call variants with only 6% recall, but 74% precision. The TMB from RNA-Seq variant calling was also validated against an external cohort made up of 11 WGS samples comprised of 9 cancer of unknown primary (CUP) and 2 MCC samples with a Pearson's correlation of 0.98. Despite the low recall rate, UV mutational signatures were still able to be identified and were dominant in the viral negative samples.

Calculation of TMB

TMB was calculated for a given sample by counting the total number of exon bases that had a coverage of 8 or more using *Mosdepth* (version 0.2.5)[11], dividing this by the total number of detected coding mutations and multiplying by 1 million (mutations/megabase).

Mutational signature generation

Mutation signatures were generated for each sample in the cohort using *MutationalPatterns*[12]. The generated signatures were then matched to the single bases substitution (SBS) signatures from COSMIC v3[13 14].

Table S1. Genes used in determining cell-type-specific gene expression. These gene sets were identified by Danaher et al[15] by using co-expression patterns from large tumor gene expression datasets to evaluate previously reported marker and gene lists.

Gene	Cell Type
BLK	B-cells
CD19	B-cells
MS4A1	B-cells
TNFRSF17	B-cells
FCRL2	B-cells
KIAA0125	B-cells
PNOC	B-cells
SPIB	B-cells
TCL1A	B-cells
PTPRC	CD45
CD8A	CD8 T cells
CD8B	CD8 T cells
CTSW	Cytotoxic cells
GNLY	Cytotoxic cells
GZMA	Cytotoxic cells
GZMB	Cytotoxic cells
GZMH	Cytotoxic cells
KLRB1	Cytotoxic cells
KLRD1	Cytotoxic cells

KLRK1	Cytotoxic cells
PRF1	Cytotoxic cells
NKG7	Cytotoxic cells
CCL13	DC
CD209	DC
HSD11B1	DC
CD244	Exhausted CD8
EOMES	Exhausted CD8
LAG3	Exhausted CD8
PTGER4	Exhausted CD8
CD163	Macrophages
CD68	Macrophages
CD84	Macrophages
MS4A4A	Macrophages
MS4A2	Mast cells
TPSAB1	Mast cells
CPA3	Mast cells
HDC	Mast cells
TPSB2	Mast cells
CSF3R	Neutrophils
S100A12	Neutrophils
CEACAM3	Neutrophils
FCAR	Neutrophils

FCGR3B	Neutrophils
FPR1	Neutrophils
SIGLEC5	Neutrophils
IL21R	NK CD56dim cells
KIR2DL3	NK CD56dim cells
KIR3DL1	NK CD56dim cells
KIR3DL2	NK CD56dim cells
NCR1	NK cells
XCL2	NK cells
XCL1	NK cells
CD3D	T-cells
CD3E	T-cells
CD3G	T-cells
CD6	T-cells
SH2D1A	T-cells
TRAT1	T-cells
TBX21	Th1 cells
FOXP3	Treg

Table S2. Hallmark gene sets. Hallmark gene sets called as significantly enriched in patients with an observable response to ICI (FDR < 0.05)**.**

Gene set	Number of Genes	Direction	*P* Value	False Discovery Rate
HALLMARK_E2F_TARGETS	199	Down	1.10E-06	5.51E-05
HALLMARK_MYC_TARGETS_V1	199	Down	4.32E-06	1.08E-04
HALLMARK_G2M_CHECKPOINT	198	Down	1.66E-04	0.00210671
HALLMARK_MTORC1_SIGNALING	198	Down	2.10E-04	0.00210671
HALLMARK_UNFOLDED_PROTEIN_RESPONSE	110	Down	2.11E-04	0.00210671
HALLMARK_OXIDATIVE_PHOSPHORYLATION	200	Down	3.71E-04	0.00309176
HALLMARK_UV_RESPONSE_UP	155	Down	0.00373543	0.02668164

Table S3. GO gene sets. Gene ontology (GO) gene sets called as significantly enriched in patients with an observable response to ICI (FDR < 0.05)**.**

Gene set	Number of Genes	Direction	*P* Value	False Discovery Rate
GO_ESTABLISHMENT_OF_PROTEIN_LOCALIZATION_TO_ENDOPLASMIC_RETICULUM	103	Down	1.18E-19	6.99E-16
GO_PROTEIN_LOCALIZATION_TO_ENDOPLASMIC_RETICULUM	122	Down	3.63E-18	1.07E-14
GO_CYTOSOLIC_RIBOSOME	107	Down	6.17E-18	1.22E-14

GO_TRANSLATIONAL_INITIATION	141	Down	3.48E-15	4.77E-12
GO_CYTOSOLIC_LARGE_RIBOSOMAL_SUBUNIT	58	Down	4.04E-15	4.77E-12
GO_NUCLEAR_TRANSCRIBED_MRNA_CATABOLIC_PROCESS_NONSENSE_MEDIATED_DECAY	115	Down	1.47E-14	1.45E-11
GO_PROTEIN_TARGETING_TO_MEMBRANE	152	Down	8.95E-14	7.56E-11
GO_RIBOSOMAL_SUBUNIT	157	Down	7.54E-13	5.58E-10
GO_MULTI_ORGANISM_METABOLIC_PROCESS	135	Down	3.36E-12	2.21E-09
GO_CYTOSOLIC_SMALL_RIBOSOMAL_SUBUNIT	41	Down	8.88E-11	5.25E-08
GO_LARGE_RIBOSOMAL_SUBUNIT	92	Down	1.29E-10	6.91E-08
GO_STRUCTURAL_CONSTITUENT_OF_RIBOSOME	198	Down	4.89E-09	2.41E-06
GO_RIBOSOME	216	Down	5.49E-09	2.50E-06
GO_IMMUNOGLOBULIN_COMPLEX	21	Down	1.35E-08	5.64E-06
GO_RNA_CATABOLIC_PROCESS	214	Down	1.43E-08	5.64E-06
GO_SMALL_RIBOSOMAL_SUBUNIT	65	Down	1.87E-08	6.92E-06
GO_CYTOSOLIC_PART	200	Down	1.77E-07	6.14E-05
GO_IMMUNOGLOBULIN_RECEPTOR_BINDING	22	Down	1.34E-06	4.41E-04
GO_KERATINIZATION	40	Up	1.73E-06	5.37E-04
GO_CORNIFIED_ENVELOPE	33	Up	3.17E-06	9.38E-04
GO_VIRAL_LIFE_CYCLE	278	Down	3.46E-06	9.68E-04
GO_ESTABLISHMENT_OF_PROTEIN_LOCALIZATION_TO_MEMBRANE	257	Down	3.60E-06	9.68E-04
GO_CHAPERONE_MEDIATED_PROTEIN_FOLDING	47	Down	4.13E-06	0.001028 65
GO_KERATIN_FILAMENT	27	Up	4.17E-06	0.001028

				65
GO_POSITIVE_REGULATION_OF_NUCLEASE_ACTIVITY	15	Down	8.69E-06	0.00205641
GO_BITTER_TASTE_RECEPTOR_ACTIVITY	20	Down	1.29E-05	0.00293593
GO_RRNA_METABOLIC_PROCESS	248	Down	1.96E-05	0.00428899
GO_PERK_MEDIATED_UNFOLDED_PROTEIN_RESPONSE	11	Down	2.57E-05	0.00542086
GO_DNA_PACKAGING_COMPLEX	57	Down	3.71E-05	0.00757515
GO_UNFOLDED_PROTEIN_BINDING	93	Down	4.23E-05	0.00834014
GO_PROTEIN_LOCALIZATION_TO_MEMBRANE	366	Down	5.14E-05	0.00952335
GO_DNA_PACKAGING	141	Down	5.15E-05	0.00952335
GO_DETECTION_OF_CHEMICAL_STIMULUS_INVOLVED_IN_SENSORY_PERCEPTION_OF_TASTE	31	Down	5.89E-05	0.0105592
GO_CYTOPLASMIC_TRANSLATION	40	Down	6.73E-05	0.01154811
GO_CELL_CYCLE_PHASE_TRANSITION	249	Down	6.83E-05	0.01154811
GO_KERATINOCYTE_DIFFERENTIATION	88	Up	8.41E-05	0.01316369

GO_INNER_MITOCHONDRIAL_MEMBRANE_PROTEIN_COMPLEX	99	Down	8.63E-05	0.013163 69
GO_PEPTIDE_CROSS_LINKING	44	Up	8.73E-05	0.013163 69
GO_PROTEIN_FOLDING_IN_ENDOPLASMIC_RETICULUM	8	Down	8.78E-05	0.013163 69
GO_ANTIGEN_BINDING	92	Down	8.90E-05	0.013163 69
GO_CENTROMERE_COMPLEX_ASSEMBLY	36	Down	9.32E-05	0.013344 39
GO_CHROMATIN_ASSEMBLY_OR_DISASSEMBLY	129	Down	9.48E-05	0.013344 39
GO_PROTEIN_DNA_COMPLEX_SUBUNIT_ORGANIZATION	181	Down	1.11E-04	0.015303 04
GO_PHAGOCYTOSIS_RECOGNITION	28	Down	1.17E-04	0.015707 39
GO_PROTEIN_FOLDING	208	Down	1.30E-04	0.017079 88
GO_PROTEIN_TARGETING	390	Down	1.47E-04	0.018889 63
GO_HUMORAL_IMMUNE_RESPONSE_MEDIATED_BY_CIRCULATING_IMMUNOGLOBULIN	52	Down	1.51E-04	0.018962 48
GO_CELL_CYCLE_G2_M_PHASE_TRANSITION	136	Down	1.68E-04	0.020646 39
GO_ORGANIC_CYCLIC_COMPOUND_CATABOLIC	396	Down	1.71E-04	0.020647

_PROCESS				68
GO_STRUCTURAL_CONSTITUENT_OF_MUSCLE	36	Up	1.90E-04	0.0223471
GO_PROTEIN_REFOLDING	19	Down	1.93E-04	0.0223471
GO_DNA_REPLICATION_INDEPENDENT_NUCLEOSOME_ORGANIZATION	41	Down	1.97E-04	0.0224258 2
GO_ESTABLISHMENT_OF_PROTEIN_LOCALIZATION_TO_ORGANELLE	348	Down	2.03E-04	0.0226745 7
GO_RESPIRATORY_CHAIN	75	Down	2.19E-04	0.0236326 1
GO_OXIDATIVE_PHOSPHORYLATION	80	Down	2.22E-04	0.0236326 1
GO_HISTONE_EXCHANGE	40	Down	2.24E-04	0.0236326 1
GO_ATP_DEPENDENT_CHROMATIN_REMODELING	61	Down	2.52E-04	0.0261378 6
GO_B_CELL_MEDIATED_IMMUNITY	81	Down	2.91E-04	0.0296602 3
GO_REGULATION_OF_NUCLEASE_ACTIVITY	23	Down	3.08E-04	0.0302431 9
GO_POLYSOME	37	Down	3.12E-04	0.0302431 9
GO_TASTE_RECEPTOR_ACTIVITY	22	Down	3.16E-04	0.0302431 9

GO_MRNA_METABOLIC_PROCESS	572	Down	3.17E-04	0.030243 19
GO_MITOCHONDRIAL_PROTEIN_COMPLEX	128	Down	3.30E-04	0.030949 74
GO_AMIDE_BIOSYNTHETIC_PROCESS	483	Down	3.36E-04	0.030949 74
GO_EPIDERMAL_CELL_DIFFERENTIATION	129	Up	3.40E-04	0.030949 74
GO_REGULATION_OF_CELL_CYCLE_G2_M_PHA SE_TRANSITION	57	Down	3.55E-04	0.031785 29
GO_NUCLEAR_ENVELOPE_REASSEMBLY	17	Down	3.64E-04	0.032123 51
GO_RIBOSOME_BIOGENESIS	295	Down	4.38E-04	0.037661 36
GO_INTERMEDIATE_FILAMENT	85	Up	4.39E-04	0.037661 36
GO_LYMPHOCYTE_MEDIATED_IMMUNITY	124	Down	4.48E-04	0.037875 36
GO_PROTEIN_LOCALIZATION_TO_ORGANELLE	533	Down	4.97E-04	0.041368 47
GO_RIBONUCLEOPROTEIN_COMPLEX	685	Down	5.24E-04	0.043009 03
GO_INTERSPECIES_INTERACTION_BETWEEN_O RGANISMS	627	Down	5.37E-04	0.043505 89
GO_MITOCHONDRIAL_ELECTRON_TRANSPORT_	15	Down	5.59E-04	0.044657

CYTOCHROME_C_TO_OXYGEN				5

References

1. Dobin A, Davis CA, Schlesinger F, et al. STAR: ultrafast universal RNA-seq aligner. *Bioinformatics* 2013;29(1):15-21.
2. Patro R, Duggal G, Love MI, et al. Salmon provides fast and bias-aware quantification of transcript expression. *Nature methods* 2017;14(4):417.
3. Soneson C, Love MI, Robinson MD. Differential analyses for RNA-seq: transcript-level estimates improve gene-level inferences. *F1000Research* 2015;4
4. Ritchie ME, Phipson B, Wu D, et al. limma powers differential expression analyses for RNA-sequencing and microarray studies. *Nucleic acids research* 2015;43(7):e47-e47.
5. Wu D, Smyth GK. Camera: a competitive gene set test accounting for inter-gene correlation. *Nucleic acids research* 2012;40(17):e133-e33.
6. Liberzon A, Subramanian A, Pinchback R, et al. Molecular signatures database (MSigDB) 3.0. *Bioinformatics* 2011;27(12):1739-40.
7. McKenna A, Hanna M, Banks E, et al. The Genome Analysis Toolkit: a MapReduce framework for analyzing next-generation DNA sequencing data. *Genome research* 2010;20(9):1297-303.
8. DePristo MA, Banks E, Poplin R, et al. A framework for variation discovery and genotyping using next-generation DNA sequencing data. *Nature genetics* 2011;43(5):491.
9. Koboldt DC, Zhang Q, Larson DE, et al. VarScan 2: somatic mutation and copy number alteration discovery in cancer by exome sequencing. *Genome research* 2012;22(3):568-76.
10. Ramaswami G, Li JB. RADAR: a rigorously annotated database of A-to-I RNA editing. *Nucleic acids research* 2013;42(D1):D109-D13.
11. Pedersen BS, Quinlan AR. Mosdepth: quick coverage calculation for genomes and exomes. *Bioinformatics* 2017;34(5):867-68.
12. Blokzijl F, Janssen R, Van Boxtel R, et al. MutationalPatterns: comprehensive genome-wide analysis of mutational processes. *Genome medicine* 2018;10(1):33.
13. Alexandrov L, Kim J, Haradhvala NJ, et al. The repertoire of mutational signatures in human cancer. *BioRxiv* 2018:322859.
14. Tate JG, Bamford S, Jubb HC, et al. COSMIC: the catalogue of somatic mutations in cancer. *Nucleic acids research* 2018;47(D1):D941-D47.
15. Danaher P, Warren S, Dennis L, et al. Gene expression markers of tumor infiltrating leukocytes. *Journal for immunotherapy of cancer* 2017;5(1):18.